Saturable and reverse saturable absorption in silver nanodots at 532 nm using picosecond laser pulses

Ullas Gurudas,[1,a)] Elijah Brooks,[1] Daniel M. Bubb,[1,b)] Sebastian Heiroth,[2,c)] Thomas Lippert,[2,d)] and Alexander Wokaun[2,e)]
[1]*Department of Physics, Rutgers–The state University of New Jersey, Camden, NJ 08102, USA*
[2]*Materials Group, Paul Scherrer Institut, CH-5232 Villigen PSI, Switzerland*

(Received 5 May 2008; accepted 11 August 2008; published online 3 October 2008)

Saturable absorption (SA) and reverse saturable absorption (RSA) at 532 nm were observed in Ag nanodots prepared by pulsed laser deposition. The real [Re $\chi^{(3)}$] and imaginary [Im $\chi^{(3)}$] parts of the third order nonlinearity of these films were measured using the *Z*-scan technique. At low input irradiances, the decrease in absorption near the focal point results from a negative Im $\chi^{(3)}$ and yields SA. At higher input irradiance, RSA becomes dominant. The transition from SA to RSA suggests that there is a threshold irradiance at which additional nonlinear process(es) is (are) involved and become dominant. The recovery time of these nonlinear processes was measured by a degenerate pump-probe experiment. The effects are explained in terms of the electron dynamics in the excited states. © *2008 American Institute of Physics*. [DOI: 10.1063/1.2990056]

I. INTRODUCTION

Noble metal nanoparticles have attracted attention in photonics research because of their potential application in devices due to large nonlinear susceptibilities and fast response time.[1–5] Metal nanoparticles have close-lying bands that allow electrons to move in a nearly free fashion. The oscillation of the free electrons in the conduction band occupying energy states near the Fermi level gives rise to surface plasmon resonance (SPR). The presence of a SPR band enhances the third order susceptibility $\chi^{(3)}$ of metal nanoparticles, which determines the suitability of the material for optical applications. The third order nonlinear polarization $P^{(3)}=\chi^{(3)}E^{(3)}$ gives rise to self-focusing, self-phase modulation, soliton propagation, and phase conjugate reflection.[6] The size and shape of the nanoparticles play a crucial role in the surface plasmon absorption band and, hence, the optoelectronic properties of these materials.[7,8]

Silver is a good choice for optical applications. Ag nanoparticles have the potential to obtain the largest enhancement factors due to the strength of the local field that gives rise to SPR (Refs. 9 and 10) and large third order nonlinearity.[4,5] Surface-enhanced optical second harmonic generation (SHG) in silver island films was observed by Wokaun *et al.*[11] The excitation of local surface plasmons in silver nanoparticles mediated the resonant enhancement of the local field and led to an increase in the SHG intensity by up to three orders of magnitude. In comparison with gold, for example, silver is also known to introduce significantly lower losses at visible frequencies.[12] The SPR energy of silver is far from the interband transition energy. This facilitates the separate investigation of nonlinear effects arising from interband transitions and those due to the SPR.

Several studies have been performed at or near the SPR wavelength for silver metal clusters to investigate their nonlinear optical behavior and ultrafast electron dynamics. Most of these studies were performed either on silver colloidal solutions or on silver doped glasses. Although intensity dependent saturable absorption (SA) and reverse saturable absorption (RSA) in silver nanoparticles at the same wavelength are reported in the literature, a quantitative analysis of these effects is still missing. In this paper, we report the observation of SA and RSA in Ag nanoparticles at 532 nm that have been deposited on quartz substrates using pulsed laser deposition. In particular, we present the measurement of the real [Re $\chi^{(3)}$] and imaginary [Im $\chi^{(3)}$] parts of the third order nonlinearity of these films and the response time of the SA and RSA processes using the *Z*-scan and degenerate pump-probe experiments, respectively.

II. EXPERIMENTAL DETAILS

The Ag nanoparticles were deposited using pulsed laser deposition on quartz substrates, as described in Ref. 13. A KrF excimer laser (Lambda Physik, Model LPX 105e, pulse width of 20 ns) operated at a repetition rate of 10 Hz was employed to ablate a rotatable cylindrical silver target (Goodfellow, 99.95%+) at a fluence of approximately 3.0 J/cm^2 in a high vacuum chamber. The evaporated material was deposited on quartz substrates mounted on a rotating sample holder positioned at a distance of 50 mm from the target in a nitrogen atmosphere of 5.0×10^{-5} mbar at room temperature. The deposition times were varied from 1 to 10 min. The absorption spectra of the Ag films were acquired using a dual beam UV-vis absorption spectrophotometer (Varian Cary 500 Scan) versus an uncoated quartz substrate as reference. Topographical images were obtained using tapping-mode atomic force microscope (AFM) (Digital Instruments Nanoscope IIIa) with a Si cantilever (k =0.35 N/m) and field emission scanning electron microscopy (SEM) (Zeiss Supra 55VP) for particle size analysis.

[a)]Electronic mail: ullasg@camden.rutgers.edu.
[b)]Electronic mail: dbubb@camden.rutgers.edu.
[c)]Electronic mail: sebastian.heiroth@psi.ch.
[d)]Electronic mail: thomas.lippert@psi.ch.
[e)]Electronic mail: alexander.wokaun@psi.ch.

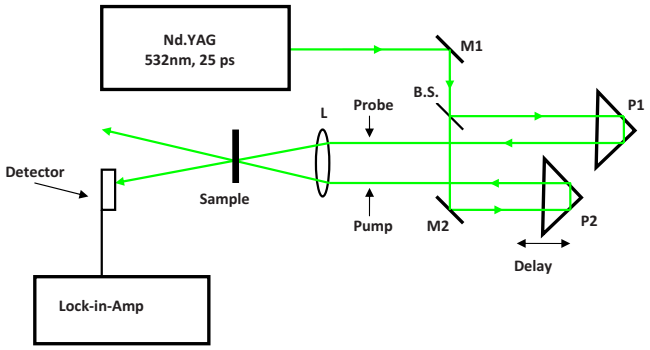

FIG. 1. (Color online) Experimental setup for the degenerate pump-probe experiment.

We employed the same experimental setup for the *Z*-scan measurement as described in the literature.[14,15] Briefly, a spatially and temporally Gaussian picosecond Nd-doped yttrium aluminum garnet laser (EKSPLA PL2241) was operated at a wavelength of 532 nm and a repetition rate of 250 Hz, and a ~25 ps pulse duration was focused to a beam waist using a 30 cm focal length lens. A detector is placed at the far field, with its output being fed to a lock-in-amplifier (Stanford Research Systems SR830) for monitoring the intensity of the laser for both closed aperture ($S=0.4$) and open aperture ($S=1$) measurements when the sample is scanned along the Z axis of the laser beam. A beam splitter directed a portion of the beam onto a reference detector whose output was monitored using an electrometer (Keithley 197A) to account for intensity fluctuations of the laser during the experiment. For the degenerate pump-probe measurement, the 532 nm laser is split into two parts with an intensity ratio of 90:10 as pump and probe, respectively, and aligned to the sample, as shown in Fig. 1. The pump beam was delayed using a high precision translation stage, and the corresponding differential transmission, $\Delta T/T(t) = (T_{on}-T_{off})/T_{off}$, was measured as a function of the temporal delay, t, using a lock-in amplifier. T_{on} and T_{off} are the probe transmittances with and without the pump, respectively. The coherent interaction of the probe with the polarization set by the pump beam when they overlap in time can be neglected because the phase relaxation time of electrons is very short in metals, and this precaution is necessary only when the detailed dynamics around a zero delay is required.[16]

III. RESULTS

The absorption spectra of the Ag nanodots prepared at different deposition times and thus with different sizes are shown in Fig. 2(a). The AFM and SEM observations of the

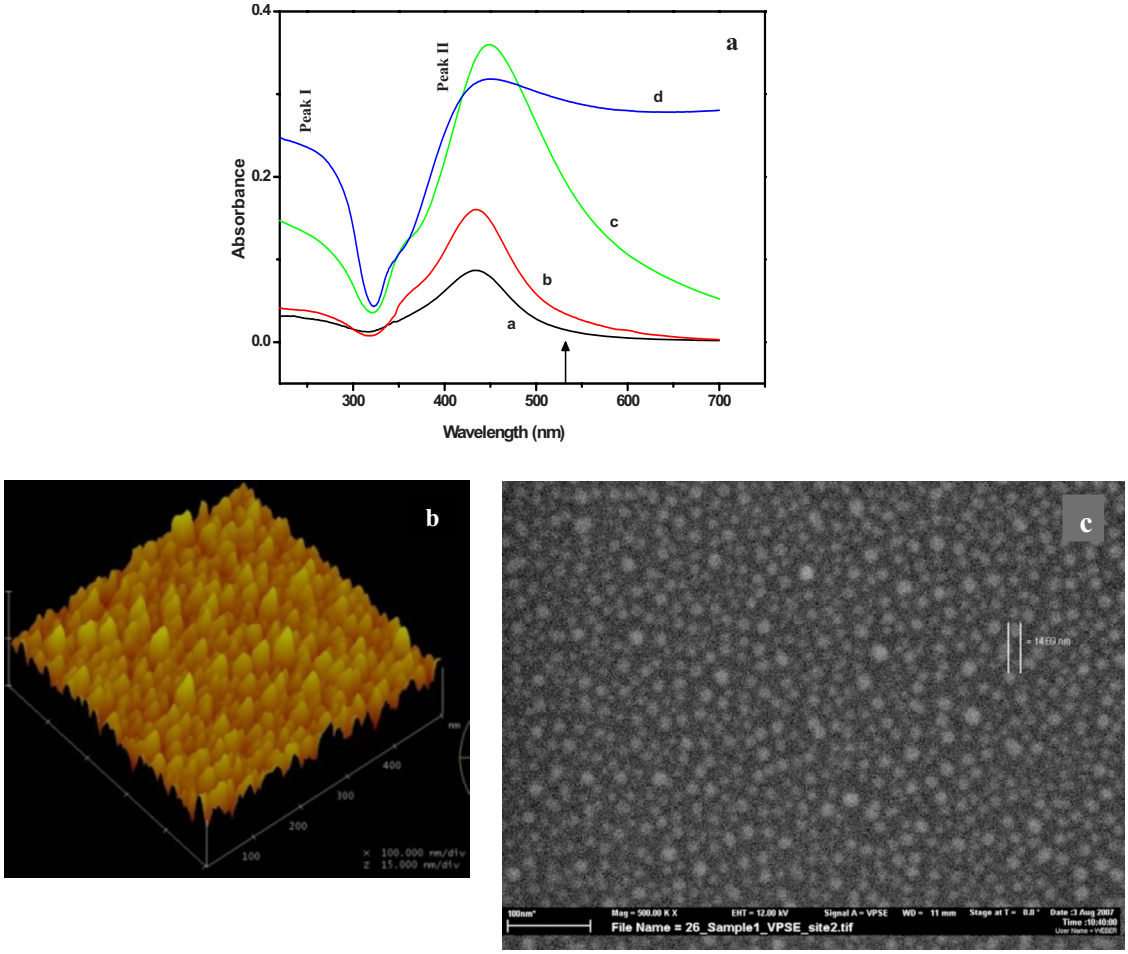

FIG. 2. (Color online) (a) Absorption spectra of silver nanodots of different particle sizes. The upward arrow corresponds to the excitation wavelength for the *Z*-scan measurement. (a) 12 nm, (b) 17 nm, (c) 20 nm, and (d) 52 nm. (b) AFM picture of silver nanodots of an average particle size of 17 nm. (c) SEM picture of silver nanodots of an average particle size of 17 nm.

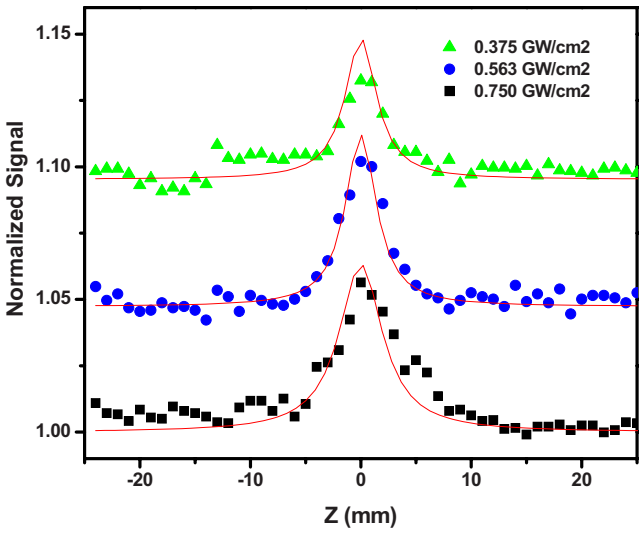

FIG. 3. (Color online) Open aperture *Z*-scan results of the Ag naonodots with an average particle size of 17 nm at low laser intensities. The solid lines are the theoretical fits to the experimental data using Eq. (4).

nanodots used for the *Z*-scan measurements are shown in Figs. 2(b) and 2(c), respectively. These measurements demonstrate that the nanoparticles have a wide range of size and spherical-like shape distribution. The average diameters of the nanoparticles prepared at 1, 2, 5, and 10 min deposition time are 12, 17, 20, and 52 nm, respectively, as evident from the AFM and SEM results. The SPR band at 410 nm increases as the deposition time increases from 1 to 5 min. The intensity of the SPR band starts to decrease, and the peak becomes broader for a deposition time of 10 min.

The experimental results of the open aperture *Z*-scan for the silver nanoparticles with an average particle diameter of 17 nm deposited on the quartz substrates at low laser excitation levels are shown in Fig. 3, which shows the negative sign for the absorption nonlinearities due to SA. The solid line is the theoretical fit to the experimental data according to Eq. (4) (see below). Figure 4(a) shows the open aperture *Z*-scan measurements on the same sample at higher laser excitation levels. As we increase the pump laser intensity, the nonlinear behavior changes from SA to RSA. Such effects were observed earlier in longitudinal SPR in gold nanoparticles[17] and copper-doped silicate glasses.[18] The reversible transformation from SA to RSA suggests that another nonlinear effect is initiated and dominates the nonlinear response of the material. Figure 4(b) depicts the transmittance of the Ag nanoparticles plotted as a function of the input irradiance. The transmittance decreases when the laser irradiance is greater than 1.3 GW/cm^2, which is a typical optical limiting. The threshold of limiting (the incident irradiance at which the nanoparticle transmittance falls to one-half of the linear transmittance[17]) for the silver nanoparticles possessing an average size of 17 nm is found to be 2.8 GW/cm^2. The transmittance of the Ag nanoparticles increases with particle size and shifts the threshold for RSA to larger laser irradiances. Figure 5 shows the open aperture *Z*-scan measurement of the films deposited for 2 and 10 min (particle sizes of 17 and 52 nm, respectively) excited at a laser irradiance of 0.75 GW/cm^2. The current study has been confined to only two particle sizes of 17 and 52 nm, mainly to focus on the eligibility of these films for various optical applications using the *Z*-scan technique. A detailed investigation of the size dependence on the various nonlinear optical parameters will be published elsewhere.

To analyze the experimental data, we used the *Z*-scan theory proposed by Sheik-Bahae *et al.*[15] The third order nonlinear susceptibility is considered to be a complex quantity,

$$\chi^{(3)} = \chi_R^{(3)} + i\chi_I^{(3)}. \tag{1}$$

Here the imaginary part of $\chi^{(3)}$ is related to the nonlinear absorption coefficient β through

$$\mathrm{Im}\,\chi^{(3)} = \frac{n_0^2 \varepsilon_0 c^2}{\omega}\beta. \tag{2}$$

The real part of $\chi^{(3)}$ is related to the nonlinear index of refraction $\gamma(m^2/W)$ through

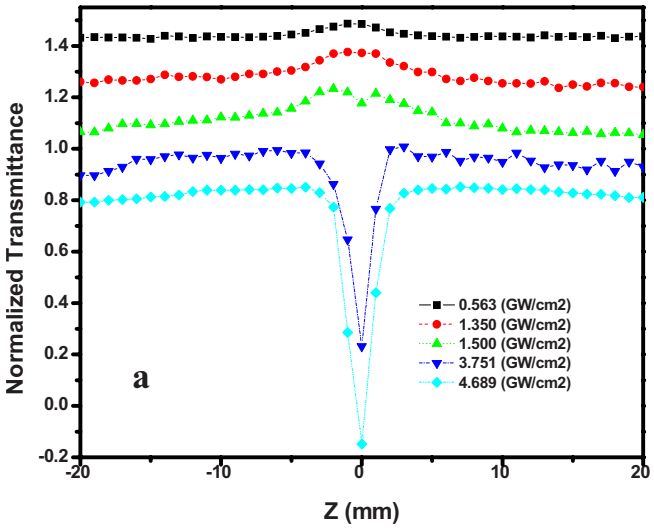

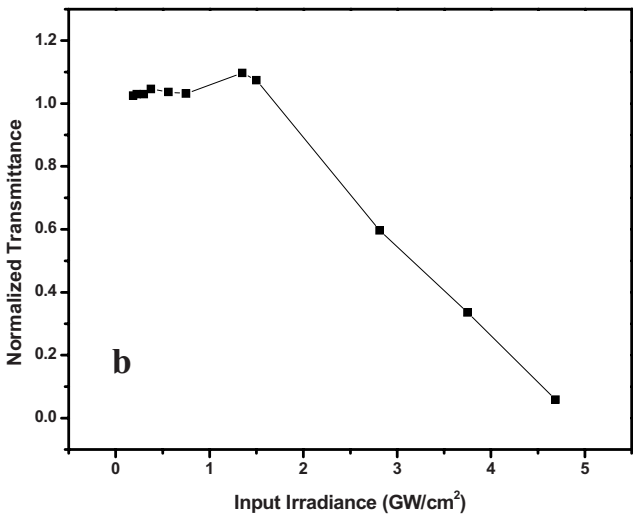

FIG. 4. (Color online) (a) Open aperture *Z*-scan results of the Ag nanodots with an average particle size of 17 nm at higher laser intensities. (b) Transmittance of Ag nanodots as a function of input laser intensity.

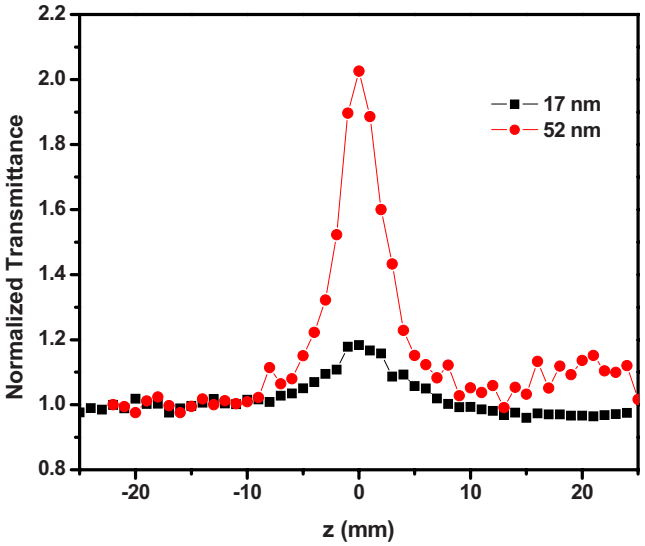

FIG. 5. (Color online) Comparison of the open aperture *Z*-scan signal for the nanodots with average particle sizes of 17 and 52 nm at an input laser intensity of 0.75 GW/cm^2.

$$\mathrm{Re}\ \chi^{(3)} = 2n_0^2\varepsilon_0 c\gamma, \tag{3}$$

where n_0 is the linear index of refraction, ε_0 is the permittivity of vacuum, ω is the optical frequency, and c is the velocity of light. The normalized transmittance can be expressed as

$$T_{\mathrm{norm}}(z) = \sum_{m=0}^{\infty} \left(\frac{-\beta I_0 L_{\mathrm{eff}}}{1+z^2/z_0^2}\right)^m /(1+m)^{3/2}, \tag{4}$$

where I_0 is the intensity of laser radiation, $L_{\mathrm{eff}} = (1-e^{-\alpha_0 L})/\alpha_0$ is the effective interaction length with the sample thickness L, α_0 is the linear absorption coefficient, and z_0 is the Rayleigh diffraction length. Typically, if $|\beta I_0 L_{\mathrm{eff}}| < 0$ is satisfied, only the first few terms are needed for a numerical evaluation.[19] Fitting the experimental data can thus give β. Once β is known, Im $\chi^{(3)}$ can also be determined. Fitting the open aperture *Z*-scan data to Eq. (4) for the film of Ag nanoparticles with an average size of 17 nm and excited at a laser irradiance of 1.43 GW/cm^2 yielded a value of $\beta = -(4.06 \pm 0.8) \times 10^{-7}$ m/W and Im $\chi^{(3)} = -(1.1 \pm 0.2) \times 10^{-10}$ esu for the nonlinear absorption coefficient and the imaginary part of the third order susceptibility, respectively. The corresponding values for the nanoparticles with an average size of 52 nm and excited at a laser irradiance of 1.43 GW/cm^2 are $\beta = -(1.55 \pm 0.02) \times 10^{-6}$ m/W and Im $\chi^{(3)} = -(4.19 \pm 0.05) \times 10^{-10}$ esu. The decrease in $|\mathrm{Im}\ \chi^{(3)}|$ as the laser intensity increases is shown in Fig. 6.

To evaluate the nonlinear refractive index γ and Re $\chi^{(3)}$, we performed a closed aperture *Z*-scan measurement on the 10 min film (average particle size of 52 nm). The closed aperture *z*-scan measurement on this film for a laser irradiance of 2.15 GW/cm^2 looked very similar to the open aperture data, but on closer examination it is revealed that the maximum transmittance occurs at $z \sim 2$ mm when we scan from an initial position of $z \sim -20$ mm. Such behavior occurs because the small aperture transmittance reflects both nonlinear absorption and nonlinear refractive effects, and the Im $\chi^{(3)}$ component dominates the Re $\chi^{(3)}$ component in the *Z*-scan transmittance curve. Similar results were reported by Hamanaka *et al.*[20] on Ag nanocrystal-glass composite samples with a sample thickness of 47 μm and an average Ag nanocrystal diameter of 7 nm using photon energies between 2.82 and 3.23 eV as the excitation source. The refractive contribution to the nonlinearity $T_{\mathrm{refr}}(z)$ was extracted from the absorptive contribution by dividing the normalized transmittance with a closed aperture $T_a(z)$ by the normalized transmittance with no aperture $T_{\mathrm{na}}(z)$ using the following equation:[21]

$$T_{\mathrm{refr}}(z) = \frac{T_a(z)}{[T_{\mathrm{na}}(z/1.25)]^p}, \tag{5}$$

where $p = S + 0.67(1-S)^2$, with S as the aperture linear transmittance defined as[15] $S = 1 - \exp(-2r_a^2/w_a^2)$, where r_a is the aperture radius and w_a is the beam radius at the aperture in the linear regime. The value of S is 0.4 in our case. The

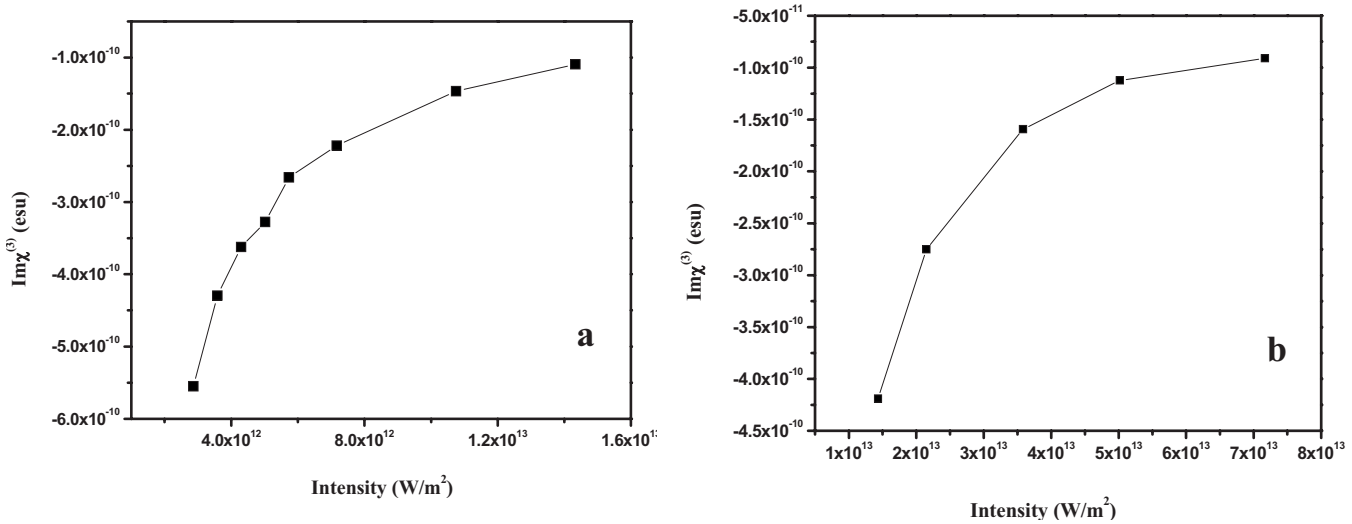

FIG. 6. (a) Variation in Im $\chi^{(3)}$ with input laser intensity for the nanodots of an average particle size of 17 nm. (b) Variation in Im $\chi^{(3)}$ with input laser intensity for the nanodots of an average particle size of 52 nm.

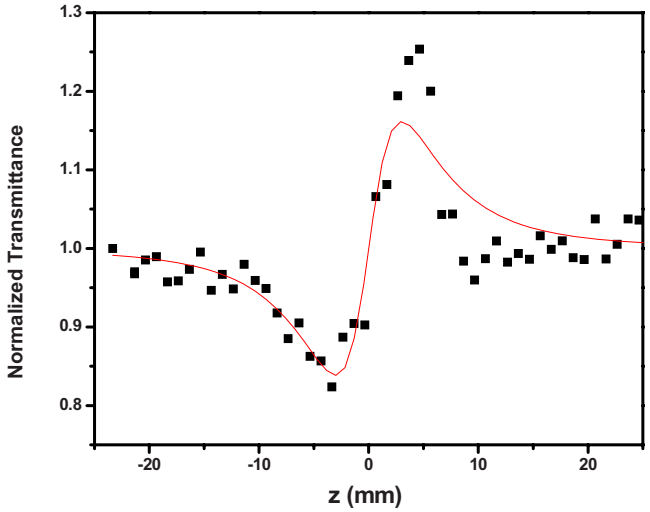

FIG. 7. (Color online) $T_{\mathrm{refr}}(z)$ derived from the open and closed aperture data using Eq. (5). The solid line is the theoretical fit using the equation given in Ref. 15.

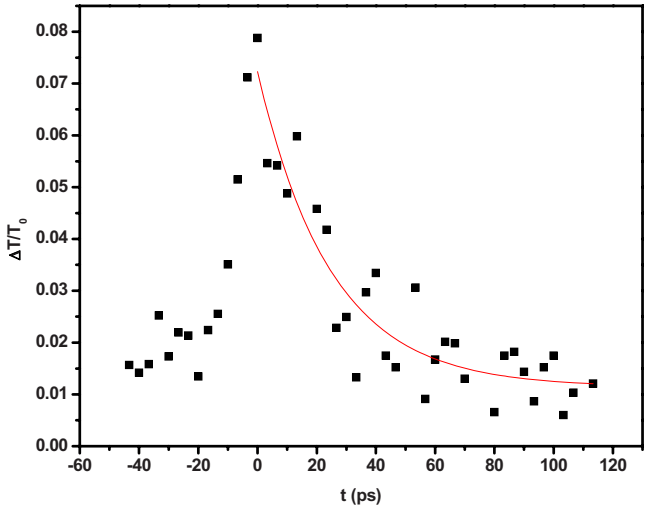

FIG. 8. (Color online) Transient transmission when only SA is present. The solid line is the best fit to the experimental data.

$T_{\mathrm{refr}}(z)$ thus derived is shown in Fig. 7. The nonlinear refractive index γ is evaluated from $T_{\mathrm{refr}}(z)$ using the formula given by Sheik-Bahae *et al.*[15] We obtained the values for $\gamma = +(6.03 \pm 0.4) \times 10^{-14}$ m^2/W and Re $\chi^{(3)} = +(3.82 \pm 2) \times 10^{-11}$ esu for the film with an average particle size of 52 nm with a laser irradiance of 2.15 GW/cm^2. Our result for Re $\chi^{(3)}$ is positive and comparable to the results reported by Hamanaka *et al.*[20] They observed a change in the sign of Re $\chi^{(3)}$ between photon energies of 2.85 and 3.23 eV. They reported values of Re $\chi^{(3)}$ for photon energies of 2.82 and 2.85 eV as negative and for 3.23 eV as positive. However, they did not report values for Re $\chi^{(3)}$ below 2.82 eV. The sign reversal of the nonlinear refractive index in Ag doped glasses was reported earlier by Osborne *et al.*[22] However, this process was irreversible due to a photochemical reaction, which produced a silver oxide layer on the surface of the Ag nanoclusters. This effect can be ruled out in our case because the *Z*-scan had excellent reproducibility. Ganeev *et al.*[23] observed a variation in γ and Re $\chi^{(3)}$ with an increase in laser intensity leading to a change in the sign of the nonlinear refractive index from negative to positive on silicate glasses doped with silver nanoparticles when using 55 picosecond laser pulses at 532 nm. Due to the low transmittance intensity and the strong contribution from the Im $\chi^{(3)}$, Re $\chi^{(3)}$ was too small to be detected in the case of the Ag film of an average particle size of 17 nm.

To evaluate the recovery time of the observed nonlinearities, we did a degenerate pump-probe experiment with 25 ps, 532 nm laser pulses. Figure 8 shows the transient absorption signals of the silver nanoparticles deposited for 2 min (particle size of 17 nm) when only SA was present. The pump laser power was kept at 0.56 GW/cm^2 to avoid RSA. The solid line is the best fit with a single exponential decay that gives a decay time of $\tau = 24.8 \pm 4$ ps . Because of the instability, we could not record the transient absorption signals at or near the zero delay when RSA was present.

IV. DISCUSSION

Optical absorption spectra of Ag nanoparticles consist of two principal peaks, as reported earlier.[8] The first is situated in the ultraviolet [peak I in Fig. 2(a)], and the second is in the visible wavelength [peak II in Fig. 2(a)] region. The peak observed in the ultraviolet wavelength region corresponds to the optical absorption originating from interband transitions. The peak observed in the visible wavelength region (peak II) arises from the SPR. The plasmon peak blueshifts and becomes narrower as the average particle size decreases. Metal nanoparticles have close-lying bands, and electrons move nearly free within them. The conduction and valance bands are divided into discrete energy levels, with the degeneracy and separation of these discrete levels depending on their shape and size.[6] The plasmon absorption is the collective oscillation of the conduction electrons on the surface of the nanoparticles. The resonance frequency of the plasmon peak is determined by the dielectric function of the metal and the surrounding medium in addition to the shape and size of the nanoparticles.[8] The Mie theory[24] and the Maxwell-Garnett theory[25] along with experimental results confirm that the peak position shifts to the red and the band broadens as the size of the nanoparticle increases. It is well known that the aggregation of small Ag particles leads to a broad plasmon absorption band across the entire visible spectrum,[25] as seen in the spectrum of the film, which has an average particle size of 52 nm in Fig. 2(a).

In the case of the noble metals, the optical properties are influenced by the localized outermost electrons in the *d*-bands and by the quasi-free-electrons in the *s-p* conduction bands. The *d*-band lies from 2 to 5 eV below the Fermi level (E_F) for almost all wavevectors k. The optical properties of noble metals in the visible range are predominantly due to these so-called interband transitions between the levels in the *d*-band that are just below the Fermi energy and the conduction band. Clusters with fewer than 100 atoms[6,19] possess this band structure. Electronic transitions between the *d*-bands and the conduction band can occur for photon energies $\hbar\omega$ larger than the energy gap at the *X*-point of the Brillouin zone. The transition threshold for Ag is 4 eV.[6]

Different processes, such as transient absorption, photoejection of electrons by a two-photon or multiphoton absorp-

tion, interband and intraband transitions, and nonlinear scattering, can lead to the nonlinear absorption in nanoclusters. For Ag, the SPR is situated well below the interband transition threshold $d \rightarrow p$ (E_{dp}=3.99 eV or 310 nm) and $p \rightarrow s$ (E_{ps}=3.85 eV or 322 nm) from the occupied p-state to the unoccupied s-state.[16,26] To induce the interband transition ($4d \rightarrow 5s$ for Ag), the photon energy has to be larger than the gap energy, which is 4.0 eV in the case of Ag.[19] In our Z-scan experiment, the excitation wavelength is 532 nm (2.33 eV), which is obviously smaller than 4.0 eV. Qu *et al.*[19] reported Z-scan studies performed on Au and Ag nanoparticles precipitated in glasses with nanosecond pulses at 532 nm. They observed RSA in the case of Ag and attributed it to the interband transition resulting from two-photon absorption. In contrast to their results, we observed SA in Ag nanoparticles deposited on a quartz substrate when excited by picosecond laser pulses at 532 nm.

The plasmon band of metal nanoparticles as explained by the Mie theory involves dipolar oscillations of the free electrons in the conduction band that occupy energy states near the Fermi level. Once these electrons are excited by a laser pulse, they do not oscillate at the same frequency as that of the unexcited electrons, thus causing the plasmon absorption band to bleach.[27] The broad nature of the plasmon band is indicative of a wide range of particle sizes and shapes. So, by changing the excitation wavelength, it is possible to selectively excite particles within a range of sizes and shapes. If we carry out the excitation at a longer wavelength such as 532 nm, we can excite Ag clusters that do not contribute to the main plasmon band. From the transient absorption studies in Ag nanoclusters, Kamat *et al.*[27] confirmed that the photophysical processes observed with 355 and 532 nm laser pulse excitations are essentially similar. The difference in their observed transient spectra from both the excitation wavelengths was due to the fact that different-sized particles are excited at different pump wavelengths.

In the case of the nanoparticles, the electron dynamics is strongly influenced by the surface at the boundary of the metal and the surrounding dielectric matrix.[16] The excited electrons relax to the ground state through electron-electron interaction (few hundred femtoseconds) and electron-phonon interactions (few picoseconds). Because of the phonon-phonon interactions, the full recovery of the ground state plasmon band is delayed further. Thus, the broad transient absorption that gains control subsides within 100 ps and gives way to a complete recovery of the bleached spectrum.[28]

The relaxation dynamics of the metal nanoclusters also depend on the energy absorbed by the nanoparticles and their size, the surrounding matrix, and the excitation wavelength. The relaxation time decreases with increasing particle diameter at higher energies and is reported to show an increase at the SPR. Faster relaxations make further excitation of the relaxed electrons and further transfer of energy via electron-electron and electron-phonon interactions possible.[26] Since the relaxation times are much shorter than the laser pulse duration in the case of the excitation with nanosecond laser pulses, individual electrons can be subjected to multiple excitation events. So, a complete bleaching of the ground state

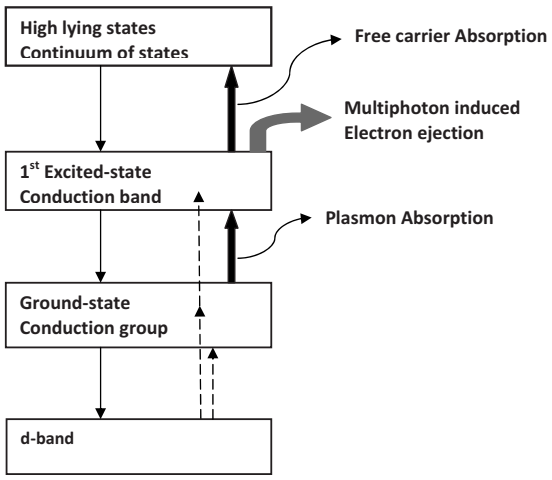

FIG. 9. Energy level diagram for the electron dynamics in Ag nanoparticles leading to SA and RSA.

may not be possible with nanosecond laser pulses of moderate powers. At higher laser intensities, free carrier absorption can also occur. The observation of RSA in the case of the excitation with nanosecond laser pulses reported in Ref. 19 may also be due to the influence of the pulse duration and/or the intensity dependent free carrier absorption. At low laser intensities (Fig. 3) in our Z-scan measurements, the 532 nm laser radiation results in an intraband electron excitation within the conduction band leading to the ground state plasmon band bleach, yielding SA. At higher laser intensities [Fig. 4(a)], the transient absorption from the free carriers becomes significant. This results in the appearance of RSA, which overrides the SA at very high intensities. In addition to the transient absorption, the photoejection of electrons may also contribute to the RSA. Visible photons are not energetic enough to directly (monophotonically) photoeject electrons, so if photoejection occurs at all it will be at higher laser intensities. This is an ultrafast process completed within the laser pulse duration.[27] The interesting property of the intensity dependent SA and RSA at the same wavelength in Ag nanodots can be used for optical pulse compression.[29] RSA can also be used as an optical limiter to protect optical sensors from high power laser pulses.

We cannot ignore interband electronic transitions due to two-photon absorption with 532 nm excitation. The wavelength range of the interband transition in Ag is located below 320 nm, so the two-photon absorption connected with interband transition can be excited with 532 nm radiation at sufficient intensity. The decrease in $|\mathrm{Im}\ \chi^{(3)}|$ shown in Fig. 6 confirms such an assumption. The possible mechanism for the decrease in $\mathrm{Im}\ \chi^{(3)}$ is the influence of nonlinear optical processes with opposite dependence on laser intensity, such as reverse saturated absorption and two-photon absorption.[23]

The possible absorption and relaxation mechanisms discussed above are shown in Fig. 9.[26,28] The solid block arrows pointing upward show the strong surface plasmon absorption and free carrier absorption, and the dotted arrow shows the weak interband and two-photon absorption. The block curved arrow shows the multiphoton induced electron ejec-

tion leading to charged nanoclusters, intermediate transient state, and photofragmentation.[27] The downward arrows represent the electron-phonon relaxation.

The negative value of Re $\chi^{(3)}$ for wavelengths $\lambda > \lambda_{SPR}$ was reported by Hamanaka *et al.*[20] In their *Z*-scan study using a 55 ps laser pulse at 532 nm on silicate glasses doped with Ag nanoparticles, Ganeev *et al.*[23] reported the sign change of Re $\chi^{(3)}$ at higher laser intensities. They attributed this change in the sign of the nonlinear refractive index to the influence of the interband transitions. The decrease in $|\text{Im}\ \chi^{(3)}|$ with laser intensity shown in Fig. 6 confirms the contribution of the interband transition in our *z*-scan signal.

In the relaxation process, the energy is transferred to the dielectric matrix as the heat diffusion from the metal to the environment, which is sensitive to the thermal conductivity of the surrounding medium.[16] This happens in a 10–100 ps time scale.[27,30] The relaxation time, 24.8 ± 4 ps, observed in the case of SA in our degenerate pump-probe experiment probably arises from the heating of the surrounding media.

In view of the results observed in the case of silver nanoparticles, we must discuss the suitability of the Ag films as optical switches. An ideal nonlinear material for an optical switching device should satisfy the following conditions: (i) The excitation time of the nonlinear effect must be less than the pulse width and the sum of the excitation, and relaxation times must be shorter than the pulse spacing, (ii) the effect of linear absorption must be weak compared to the effect of nonlinearity, and (iii) the effect of two-photon absorption must be weak compared to the nonlinear effect.[31] Interband and intraband electron transitions by the absorption of laser pulse happens in a few femtoseconds, so the first condition is satisfied in metal nanoparticles. The second condition is quantified in terms of the Stegeman figure of merit[32] as follows:

$$W = \frac{\Delta n_{\max}}{\alpha\lambda} > 1, \tag{6}$$

where $\Delta n_{\max}$ is the maximum obtainable refractive index change, α is the linear absorption coefficient, and λ is the wavelength. Since $\Delta n_{\max} = \gamma I_{sat}$, where I_{sat} is the light intensity at which the refractive index change saturates and γ is the nonlinear refractive index,[33] W can be written as

$$W = \frac{\gamma I_{sat}}{\alpha\lambda} > 1. \tag{7}$$

The ratio of the linear absorption coefficient α to the saturated light intensity I_{sat} can be represented as the nonlinear absorption coefficient β.[23] The figure of merit W thus simplifies as follows:

$$W = \frac{\gamma}{\beta\lambda} > 1. \tag{8}$$

In our case, the value of β and γ are $-(1.02 \pm 0.2) \times 10^{-6}$ m/W and $+(6.03 \pm 0.4) \times 10^{-14}$ m^2/W, respectively, for the film deposited for 10 min (average particle size of 52 nm) with a laser intensity of 2.15 GW/cm^2. So, the value of W is 0.11, which is way short for the required condition.

The third condition is quantified in terms of the Stegeman figure of merit,

$$T = \frac{2\beta\lambda}{\gamma} < 1. \tag{9}$$

In our case, $T = 18$ for the above sample, which is again way short for the required condition. From these calculations, we can conclude that these samples are not suitable for optical switching devices at 532 nm. However, Ganeev *et al.*[34] reported the figure of merit T for silver doped silicate glasses at 1064 nm fall in the chosen limit because of the absence of the nonlinear absorption. Strong two-photon absorption that may accompany a large nonlinear refractive index can hamper all optical switching in any material.[35] Studies in which the excitation wavelength is in the near infrared region are in progress.

V. CONCLUSIONS

In this paper we report the observation of intensity dependent SA and RSA at 532 nm in silver nanodots prepared by pulsed laser deposition. To the best of our knowledge, this is the first observation of SA and RSA at the same wavelength in the case of silver nanoparticles. The SPRs in silver nanodots were confirmed using UV-vis absorption spectroscopy, and the particle size distribution was determined using AFM and SEM. The real and imaginary parts of the third order nonlinearities of these films were measured using the *Z*-scan technique. The broad absorption in the SPR indicates that different-sized and -shaped nanoparticles are present in the samples used in the present study and that laser can selectively excite the nanoparticles within a range of sizes and shapes. The SA and RSA efficiencies at 532 nm are found to be dependent on sample properties. These processes are also found to be reversible. So by properly designing different sizes and shapes of these nanoparticles, it may be possible to use these materials for various optical applications such as laser pulse compression and optical limiting for protecting optical sensors from high power laser pulses. The results of the figure of merits W and T observed from the present measurements indicate that Ag nanoparticle films are not suitable for optical switches at 532 nm.

ACKNOWLEDGMENTS

D. M. Bubb acknowledges a Cottrell College Award from Research Corporation and Award Nos. DMI-0613837 and CMMI-0727713 from NSF. Travel costs associated with this work were funded by an International Research and Engineering Education subaward from NSF.

[1] S. Ding, X. Wang, D. J. Chen, and Q. Q. Wang, Opt. Express **14**, 1541 (2006).
[2] D. Richard, P. Roussignol, and C. Flytzanis, Opt. Lett. **10**, 511 (1985).
[3] Q. F. Zhang, W. M. Liu, Z. Q. Xue, J. L. Wu, S. F. Wang, D. L. Wang, and Q. H. Gong, Appl. Phys. Lett. **82**, 958 (2003).
[4] I. Tanahashi, H. Inouye, and A. Mito, Jpn. J. Appl. Phys., Part 1 **42**, 3467 (2003).
[5] G. Yang, D. Y. Guan, W. T. Wang, W. D. Wu, and Z. H. Chen, Opt. Mater. (Amsterdam, Neth.) **25**, 439 (2004).
[6] L. Yang, D. H. Osborne, R. F. Haglund, Jr., R. H. Magruder, C. W. White, R. A. Zuhr, and H. Hosono, Appl. Phys. A: Mater. Sci. Process. **62**, 403

(1996).
[7]S. Sun, C. B. Murray, D. Weller, L. Folks, and A. Moser, Science **287**, 1989 (2000).
[8]B. Balamurugan and T. Maruyama, J. Appl. Phys. **102**, 034306 (2007).
[9]A. Heilmann, A. Kiesow, M. Gruner, and U. Kreibig, Thin Solid Films **343–344**, 175 (1999).
[10]W. P. Cai, H. Hofmeister, and T. Rainer, Physica E (Amsterdam) **11**, 339 (2001).
[11]A. Wokaun, J. G. Bergman, J. P. Heritage, A. M. Glass, P. F. Liao, and D. H. Olson, Phys. Rev. B **24**, 849 (1981).
[12]P. B. Johnson and R. W. Christy, Phys. Rev. B **6**, 4370 (1972).
[13]T. Yamamoto, K. Machi, S. Nagare, K. Hamada, and M. Senna, Solid State Ionics **172**, 299 (2004).
[14]M. Sheik-Bahae, A. A. Said, and E. W. Van Stryland, Opt. Lett. **14**, 955 (1989).
[15]M. Sheik-Bahae, A. A. Said, T.-H. Wei, D. J. Hagen, and E. W. Van Stryland, IEEE J. Quantum Electron. **26**, 760 (1990).
[16]J.-Y. Bigot, V. Halte, J.-C. Merle, and A. Daunois, Chem. Phys. **251**, 181 (2000).
[17]H. I. Elim, J. Yang, J.-Y. Lee, J. Mi, and W. Ji, Appl. Phys. Lett. **88**, 083107 (2006).
[18]R. A. Ganeev, A. I. Ryasnyansky, A. L. Stepanov, and T. Usmanov, Phys. Status Solidi B **241**, R1 (2004).
[19]S. Qu, Y. Zhang, H. Li, J. Qiu, and C. Zhu, Opt. Mater. (Amsterdam, Neth.) **28**, 259 (2006).
[20]Y. Hamanaka, A. Nakamura, N. Hayashi, and S. Omi, J. Opt. Soc. Am. B **20**, 1227 (2003).
[21]P. B. Chapple, J. Staromlynska, J. A. Hermann, T. J. McKay, and R. G. McDuff, J. Nonlinear Opt. Phys. Mater. **6**, 251 (1997).
[22]D. H. Osborne, R. F. Haglund, Jr., F. Gonella, and F. Garrido, Appl. Phys. B: Lasers Opt. **66**, 517 (1998).
[23]R. A. Ganeev, A. I. Ryasnyansky, A. L. Stepanov, and T. Usmanov, Opt. Quantum Electron. **36**, 949 (2004).
[24]G. Mie, Ann. Phys. **330**, 377 (1908).
[25]U. Kreibig and M. Vollmer, *Optical Properties of Metal Clusters* (Springer, Berlin, 1995).
[26]P. P. Kiran, B. N. S. Bhaktha, D. N. Rao, and G. De, J. Appl. Phys. **96**, 6717 (2004).
[27]P. V. Kamat, M. Flumiani, and G. V. Hartland, J. Phys. Chem. B **102**, 3123 (1998).
[28]R. Philip, G. R. Kumar, N. Sandhyarani, and T. Pradeep, Phys. Rev. B **62**, 13260 (2000).
[29]Y. B. Band, D. J. Harter, and R. Bavli, Chem. Phys. Lett. **126**, 280 (1986).
[30]T. S. Ahmadi, S. L. Logunov, and M. A. El-Sayed, J. Phys. Chem. **100**, 8053 (1996).
[31]L. Brozozowski and E. H. Sargent, J. Mater. Sci.: Mater. Electron. **12**, 483 (2001).
[32]G. I. Stegeman, Proc. SPIE **1852**, 75 (1993).
[33]M. Samoc, A. Samoc, B. Luther-Davies, J. Swiatkiewicz, C. Q. Jin, and J. W. White, Opt. Lett. **20**, 2478 (1995).
[34]R. A. Ganeev, A. I. Ryasnyansky, A. L. Stepanov, and T. Usmanov, Phys. Status Solidi B **241**, 935 (2004).
[35]V. Mizrahi, K. W. DeLong, G. I. Stegeman, M. A. Saifi, and M. J. Andrejco, Opt. Lett. **14**, 1140 (1989).